ADDIS ABABA UNIVERSITY

SCHOOL OF GRADUATE STUDIES

DEPARTMENT OF CHEMISTRY

KINETICS OF ADSORPTION/DESORPTION OF 1-BUTYL-3-METHYLIMIDAZOLIUM BROMIDE INTO/OUT OF MORDENITE

By: Yewilsaw Chanie

Advisor: Dr. Eduardo Pérez

A THESIS SUBMITTED TO THE DEPARTMENT OF CHEMISTRY IN PARTIAL FULFILMENT OF THE REQUIREMENT OF MASTER SCIENCE DEGREE IN CHEMISTRY (PHYSICAL CHEMISTRY)

February, 2014

ADDIS ABABA UNIVERSITY

SCHOOL OF GRADUATE STUDIES

DEPARTMENT OF CHEMISTRY

KINETICS OF ADSORPTION/DESORPTION OF 1-BUTYL-3-METHYLIMIDAZOLIUM BROMIDE INTO MORDENITE

By: Yewilsaw Chanie

Approved by the Examining Board:

Dr. Eduardo Pérez (Advisor) _____

Dr. Mesfin Redi (Examiner) _____

Date: _____

January, 2014

Table of Contents

ACKNOWLEDGMENT

I would like to express my profound sense of gratitude and respect to my advisor Dr. Eduardo Pérez for his wholehearted advice. I have been extremely lucky to have a supervisor who cared so much about my work, and who responded to my questions and queries so promptly.

Next, I would like to offer my special thanks to Prof. Isabel Diaz for her assistance and material aid. Her suggestions were so valuable for our work.

I am also thankful to Dr. Yonas Chebude for allowing us to use his laboratory and materials for our work.

Assistance given by Prof. Wendimagegn Mammo and Mr. Wondimagegne Mamo was greatly acknowledged.

I am also very grateful to Dr. Ahmed Mustefa for providing facilities required for my thesis.

My special thanks are also extended to Prof. Martyn Poliakoff, Prof. Peter Licence, and Dr. Andinet Aynalem (University of Nottingham) and Ms Isabel Diaz (CSIC, Madrid) for their help with the characterization.

I would like to acknowledge my family and all my friends for their unreserved support.

Finally, I would like to acknowledge Addis Ababa university Department of Chemistry, Ministry of Education, Spanish Research council (CSIC), and University of Nottingham for their institutional and financial support.

ABSTRACT

The adsorption and desorption kinetics of ionic liquid (1-butyl-3-methylimidazolimu bromide) on mordenite have been studied. Adsorption and desorption of ionic liquid into/out of calcined and uncalcined mordenite was achieved by putting ionic liquid and mordenite in contact at 100 °C. Mordenite (synthetic) was pre-treated by calcinations at 550 °C in order to transform the terminal ammonium groups by proton groups. The adsorption of ionic liquid into mordenite was characterized using TGA and FT-IR, and quantitatively determined using CHN elemental analysis. The proportion of ionic liquid into mordenite was obtained from the percent by mass of nitrogen (% N_2) from the elemental analysis. The kinetics of adsorption and desorption was studied based on the results obtained for % N_2 composition. In addition, the kinetics of adsorption was analyzed using Lagergen pseudo first and pseudo second order kinetic models. The TGA result showed a 4% weight loss between 100 – 200 °C and 17% weight loss around 400 °C (around the), which are attributed to the weight loss of water and thermal decomposition of pure ionic liquid, respectively. The result obtained from the CHN elemental analysis showed that much of ionic liquid adsorbed into Mordenite very fast, within an hour, and reached equilibrium at 16% of $[BMIM]^+$ $[Br]^-$. On the other hand, desorption occurs much slowly, in 24 hr, and only 9% of ionic liquid was desorbed at equilibrium, suggesting that the interaction of $[BMIM]^+$ $[Br]^-$ and mordenite is significantly strong. The adsorption isotherm data fitted best with Lagergen pseudo second order kinetic model, indicating that the concentrations of both ionic liquid and mordenite are involved in the rate determining steps. The equilibrium amount of ionic liquid adsorbed into Mordenite obtained from fit, 158.2 ± 0.8 mg/g, which is very close to the value found from elemental analysis, 160.8 mg/g, further confirming the binuclear nature of the adsorption process.

LIST OF ABBREVIATIONS

5-HMF.....5-hydroxymethylfurfural

% [BMIM] [Br].....percent by mass of 1-butyl-3-methylimidazolium bromide

% C.....percent by mass of carbon

% N.....percent by mass of nitrogen

% wt.....percent by weight

ads.....adsorption

ATR.....Attenuated total reflectance

[BMIM] [Br].....1-butyl-3-methylimidazolium bromide

CHN analysis.....carbon, hydrogen, and nitrogen analysis

CHNS-elemental analyzer.....carbon, hydrogen, nitrogen and sulphur analyzer

FT-IR.....Fourier Transformed Infrared

IL(s).....Ionic Liquid(s)

IL-MOR.....Ionic Liquid with mordenite

LFO.....Lagergen Pseudo First Order kinetic model

MOR.....Mordenite

PSO.....Pseudo Second Order kinetic model

TCE.....1, 1, 1-trichloroethane

TGA.....Thermalgravimetric analysis

LIST OF SCHEMES

LIST OF FIGURES

1. INTRODUCTION

Sustainability is an emerging global issue of importance to all humanity. To address this issue, major efforts have been directed at developing effective pathways to convert non edible plant biomass into biofuels and/or feedstock chemicals, as this biomass conversion process holds promise to provide humanity with a sustainable source of fuels, materials and chemicals, once it becomes technologically and economically competitive compared to traditional oil refinery. In this context, 5-hydroxymethylfurfural (HMF), a dehydration product from fructose or glucose, has been identified as a biomass platform chemical and key bio-refining building block from plant biomass to bio-based sustainable polymers and promising biofuels such as 2,5-dimethylfuran[1].

Though many catalysts have been developed for the dehydration reaction of carbohydrates to produce HMF, it is still highly desirable to develop efficient and cheap heterogeneous catalysts for producing HMF from carbohydrates[2]. The ease of separation and recycling of the catalyst from the reaction mixture make heterogeneous catalysts to have unique opportunities for sustainable chemical processes. This can be achieved by using highly porous catalysts, displaying very large accessible surface areas. However, the increased surface area in nano-porous materials is often counteracted by the slower diffusion of reactants and products through the catalytic material[3].

Recently, biomass conversion based on Zeolites and zeotypes catalysis is an alternative approach in the presence of ionic liquids[4,5].Ionic liquid solvents are a promising new approach in the pretreatment of lignocellulosic material because of their ability to dissolve large amounts of cellulose at considerably mild conditions with close to 100% recovery. Due to the capacity of dissolution of glucose, and their intrinsic properties such as negligible vapour pressure, nonflammability, and thermal stability ionic liquids are used increasingly as solvents in biomass conversion[6].

High yield of 5-HMF (>90%) was reported in the presence of ionic liquids as a solvent with $CrCl_2$ as the Lewis acid catalyst[7]. 1-butyl-3-methylimidazolium bromide was reported that it

improved the yield of furfural during conversion of xylose in the presence of N,N-dimethylacetamide (DMA) using $CrCl_2$ as catalyst[8].

In our group, conversion of glucose and fructose into 5-HMF using zeolites and zeotypes as catalyst and ionic liquids as solvents is investigated4. One particular study focused on using mordenite as a catalyst for the conversion of glucose into 5-HMF and ionic liquid (1-butyl-3-methylimidazolium bromide) as a solvent5.

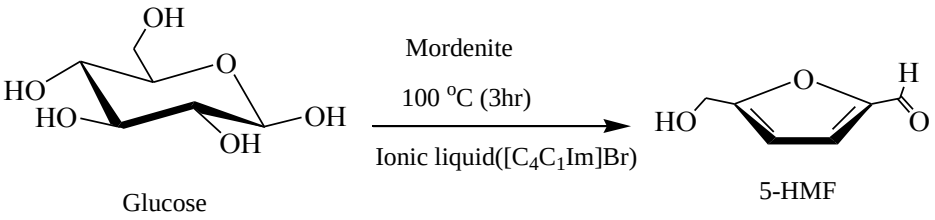

Scheme 1.1: Conversion of glucose into 5-HMF using [BMIM] [Br] as a solvent and mordenite as a catalyst.

Mordenite is a high-silica (Si/Al =10.5) zeolite characterized by channel-like framework building up the orthorhombic crystal structure[9]. Mordenite is generally regarded as a mono-dimensional zeolite, which is widely used in catalysis, separation and purification because of its uniform, small pore size, high internal surface area, flexible framework, and controlled chemistry[10]. Mordenite zeolites with moderate acidity have shown promising fructose conversion with maximum selectivity to 5-HMF (90%)[11].

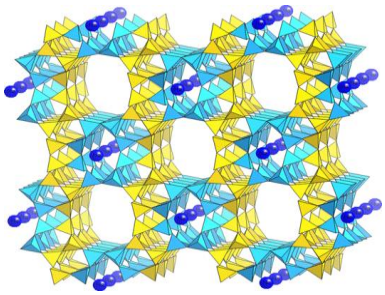

Fig.1.1. Three-dimensional Structure of mordenite

However, the attempts made were not as successful as expected; *i.e.* the yield of 5-HMF was too low (>10%) despite glucose conversion is high (>90%). The TGA result of the recovered catalyst showed a weight significant loss around 300 °C, which is attributed to the decomposition of the

ionic liquid $[BMIM]^+[Br]^-$. Investigating the causes of these results, it was realized that there is a lack of information regarding the mechanisms of the interaction between ionic liquids and zeolites including the process related to diffusion, adsorption, desorption, etc. Therefore, the major objective of this work is to investigate the efficiency of adsorption/desorption processes of the ionic liquid (1-butyl-3-methylimidazolium bromide) onto/from mordenite (channel like, one dimensional, high silica ratio Si/Al = 10.5), zeolite through the kinetic studies, since the above mentioned processes may affect the catalytic property of the zeolite significantly.

2. Literature Review

2.1. Ionic liquids

Ionic liquids are a class of organic salts, comprised entirely of cations (usually organic) and anions (usually inorganic) (see figure 2.1). Unlike molten salts such as sodium chloride which is an ionic liquid at high temperatures, room temperature ionic liquids exist as liquids at relatively low temperatures. Ionic liquids are not new: some of them have been known for many years, for instance [$EtNH_3$] [NO_3], which has a melting point of 12 °C, was first described in 1914. However, this ionic liquid did not attract further application-based research due to its explosive nature[12,13].

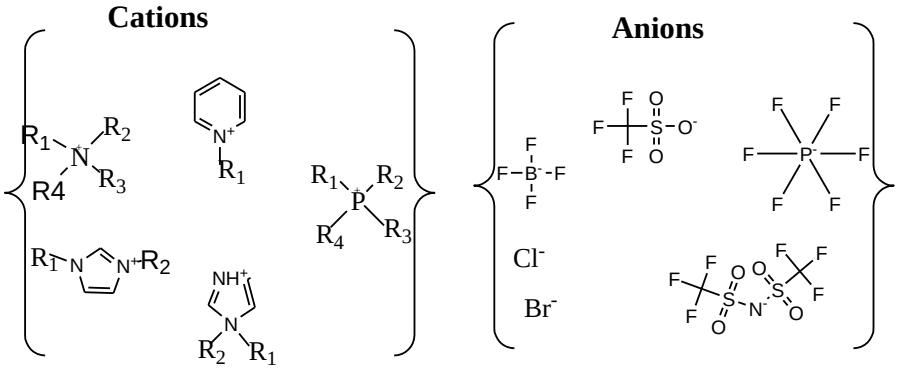

Figure 2.1: Common anions and cations of ionic liquids.

Today, ionic liquids are recognized as one of the most promising green chemical solvents due to their desirable properties. Owing to their non-volatile and non-flammable properties, they are considered ideal replacements for conventional environmentally harmful molecular solvents which are used in catalytic and organic reactions. They have a wide liquid range (for example $[BMIM]^+$ $[Cl]^-$has a melting point of 41 °C and decomposition temperature of 254 °C[14]. The asymmetric nature of the ions prevents compact packing of the ions, and makes them very useful in reactions which require both high and low temperatures. Other beneficial properties of ILs include their high thermal stability, high ionic conductivity, large electrochemical window, miscibility, water stability, density, viscosity, polarity and refractive index[15,16,17].Referred to as "designer solvents", Ionic liquid's chemical and physical properties can be adjusted and set by using different anion and cation combinations[18].

Ionic liquids appear to be highly polar due to their ionic character, resulting in their enhanced biopolymer dissolving capacity. Cellulose is insoluble in water and most common organic solvents unless using dilute sulfuric acid and high temperatures. However, it is soluble in alkyl-methylimidazolium ILs[19,20]. They can therefore be used as solvent in cellulose depolymerization and subsequent conversion of hexoses into useful platform compounds such as 5-hydroxymethylfurufral (5-HMF)[19]. Glucose can be effectively converted to HMF by CrCl2in ionic liquid solvents[21,22]such as 1-ethyl-3-methylimidazolium chloride ([EMIM]Cl) at 100 °C. Due to the catalytic advantages of zeolites as heterogeneous catalysts, nowadays, ionic liquids were reported in a biomass conversion together with zeolites[23].

2.2. Zeolites

Zeolites are crystalline, microporous three dimensional aluminosilicates of the alkali (mainly Na and K) and alkaline-earth (Ca) metals. Their crystal structure is based on a three dimensional framework of (Si/Al) O_4tetrahedra with all four oxygen shared by adjacent tetrahedral. As the result, they have a channel structure with molecular dimensions of 3 to 10Å. Because some of the $Si^{4+}$are substituted by Al^{3+}, there is a net negative charge which is balanced by extra-framework exchangeable cations mainly Na^{+}, K^{+}, Ca^{2+}, Mg^{2+}, etc.[24].

The easy and low-cost synthesis methods provide a wide variety of zeolites available for scientific and industrial purposes[25].The physicochemical properties of zeolites can be directly related to the chemical composition and crystal structure of individual species. The wide range of pore sizes available, coupled with their tuneable acidity made zeolites interesting as acid catalysts. The acidity of zeolites is directly related to the compositions of Si to Al ratio and which can be tailored. Zeolites have numerous characteristic properties that are important for commercial applications, including: high degree of hydration; low density and large pore volume when dehydrated; stability of the crystal framework structure after dehydrated; cation exchange properties; uniform molecular-sized channels in the dehydrated crystals; ability to absorb gases and vapours; catalytic properties with H^{+} exchanged forms; special electrical properties etc. [26].

Due to their excellent selectivity of zeolites to different adsorbates they are used for environmental remediation. Most of the reported applications have been focused on the removal of ammonium and heavy metal due to their high selectivity for cations and cation exchange

properties. Many industrial activities, particularly petroleum industries, introduce poisonous wastes such as volatile organic compounds and toxic anions such as chromate, nitrate, and arsenate into water bodies and wastewater streams and zeolites are widely used for purification of such pollutant[27].

Recently, biomass conversion based on zeolite catalysis is an alternative approach especially for lignocelluloses conversion to fuels. Their unique properties over other solid catalysts make them useful in shape selectivity of biomass. The micro-porous system of zeolites has an important feature to zeolites, namely shape-selectivity. The size restraints of the micropore channels can in some cases restrict the formation of large and unwanted products[28].Zeolites can be used as a heterogeneous catalyst[27] and due to ease of separation and recycling of the catalyst from the reaction mixture make heterogeneous catalysts to have unique opportunities for sustainable chemical processes areas[29]. The protic forms of zeolites are powerful solid-state acids, and can facilitate a host of acid-catalyzed reactions, such as isomerisation, alkylation and cracking[30].

2.3. Adsorption

Adsorption is The surface retention of solid, liquid, or gas molecules, atoms, or ions by a solid or liquid, as opposed to absorbtion, the penetration of substances into the bulk of the solid or liquid[31].The solid that adsorbs a component is called the adsorbent, and the component adsorbed is called adsorbate. The adsorption process is a result of interaction between the adsorbate molecules and the surface (or pore wall) of the adsorbent. The selective transfer of some of the molecules of a mixture to the surface or into the bulk of a solid (or liquid) is called sorption. The term sorption is used in a more general sense and includes both adsorption and absorption. When the sorbed molecules or atoms remain concentrated or accumulated at or near the surface, the process is called adsorption. But if these sorbed molecules are distributed throughout a liquid phase, the process is called absorption. The uptake of a gas or a liquid by a polymer is also sorption. The adsorption phenomenon provides an excellent method of separation of a variety of fluid mixtures, particularly at low concentrations, and as such it is recognized as an important mass transfer operation. It may be noted that adsorption may occur on a liquid surface too, but it is of less practical importance than adsorption in a solid.

Adsorption of a substance on a solid surface occurs because of an affinity of the surface for the particular substance. It is natural that the surface will have varying affinity for different substances. For example, activated alumina has a strong affinity for moisture, but not for hydrocarbons. Thus, a judiciously selected adsorbent preferentially adsorbs the targeted compounds from a mixture thereby acting as a medium of separation[32].

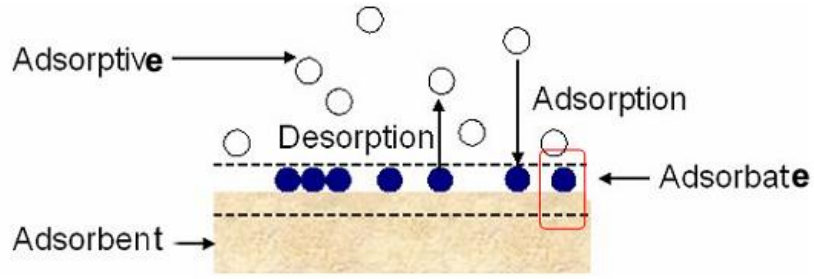

Fig. 2.2: An illustrative of adsorption-desorption processes.

Adsorption depends on the existence of a force at the surface of a solid, which reduces the potential energy of an adsorbed molecule below that of the ambient fluid phase. Generally adsorption processes can be classified in two types: physical adsorption (physisorption) and Chemisorption, depending on the nature of the surface forces.

2.3.1. Physisorption

The forces of physisorption consist of the ubiquitous dispersion-repulsion forces (Van der Waal's forces), which are a fundamental property of all mater, supplemented by various electrostatic contributions (polarization, field-dipole and field gradient-quadrupole interactions), which can be important or even dominant for polar adsorbents. The forces involved in chemisorptions are much stronger and involve a substantial degree of electron transfer or sharing, as in the adsorption energies are generally substantially greater than those for physisorption.

2.3.2. Chemisorption

Chemisorption by its very nature is limited to less than monolayer coverage of the surface whereas, in physical adsorption, multilayer adsorption is common. In a microporous solid the ultimate capacity for physisorption corresponds to the specific micropore volume, which is generally much larger than the monolayer coverage[33].

2.3.2.1. Comparison between Physisorption and Chemisorption

In the following table the major features that characterises physiosorption and chemisorption are summarized.

Table 1: Comparison between physisorption and chemisorption

Physisorption	Chemisorption
Low heat of adsorption (8-25 kJ/mol)	High heat of adsorption (~400kJ/mol)
Force of attraction are van der Waal's forces	Forces of attraction are chemical bond forces
It is reversible	It is irreversible
It is usually takes place at low temperature and decreases with increasing temperature	It takes place at high temperature
It forms multi-molecular layers	It forms monomolecular layers
It doesn't require any activation energy	It requires high activation energy
It is not very specific	It is highly specific
Rate of adsorption is very rapid	Rate of adsorption is slow
Rate of desorption is close to the rate of adsorption	Rate of desorption is much greater than the rate of adsorption
$\Delta_{ads}G^0 < 40$ kJ/mol	$\Delta_{ads}G^0 > 40$ kJ/mol

The interaction of a molecule with a given surface will also clearly be dependent upon the presence of any existing adsorbed species, whether these be surface impurities or simply pre-adsorbed molecules of the same type (in the latter case we are starting to consider the effect of surface coverage on the adsorption characteristics).

In the case of physisorption, the only attraction between the adsorbing species and the surface arises from weak, van der Waal's forces.

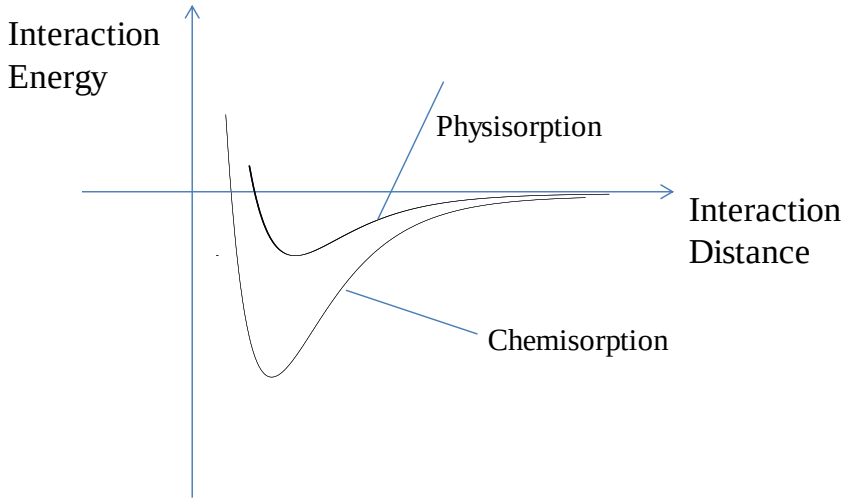

Fig. 2.3: Potential against inter-particle distance for physisorption and chemisorptions

The graph above shows the potential energy curves due to physisorption and Chemisorption separately-in practice, the potential energy curve for any real molecule capable of undergoing Chemisorption is best described by a combination of the two curves, with a curve crossing at the point at which Chemisorption forces begin to dominate over those arising from physisorption alone.

The depth of the Chemisorption well is a measure of the strength of binding to the surface - in fact it is a direct representation of the energy of adsorption, whilst the location of the global minimum on the horizontal axis corresponds to the equilibrium bond distance (r_e) for the adsorbed molecule on this surface.

Adsorption depends on both the type of adsorbent and adsorbate, more significantly, the type of adsorbent. The following three important attributes of an adsorbent make it suitable and effective for separation of a mixture: (i) selectivity, (ii) adsorption capacity, and (iii) reversibility of adsorption. The other important characteristics of an adsorbent are: (a) particle size and its distribution, (b) porosity and pore-size distribution, (c) specific surface area, and (d) structural strength and stability. A good adsorbent must have a high porosity and a narrow pore-size distribution. The last factor is especially important for size-selective adsorbents like zeolites[32].

2.3.3. Adsorption isotherms

Adsorption is usually described through an isotherm. The adsorption isotherm indicates how the adsorbed molecules distribute between the liquid phase and the solid phase when the adsorption process reaches an equilibrium state. Several models describe the process of adsorption. Over the years, a wide variety of equilibrium isotherm models (Langmuir, Freundlich, Brunauer–Emmett–Teller, Redlich–Peterson, Dubinin–Radushkevich, Temkin, Toth, Koble–Corrigan,Sips, Khan, Hill, Flory–Huggins and Radke–Prausnitz isotherm),have been formulated. Although many theories of adsorption have been put forward to explain the phenomena of adsorption, the isotherms of Freundlich and Langmuir have been widely used. Freundlich and Langmuir isotherms are of course used in adsorption to understand the extent and degree of favourability of adsorption[34].

2.3.3.1. Langmuir adsorption isotherm

The widely used Langmuir isotherm has found successful application in many real sorption processes. Langmuir adsorption isotherm, originally developed to describegas–solid-phase adsorption onto activated carbon, has traditionally and is expressed as:

$$q_e = \frac{q_\infty K_{\text{ads}} C_e}{1 + K_{\text{ads}} C_e} \qquad (1)$$

Where q_e is the adsorption density at equilibrium (kg/kg), q_∞ is the adsorption capacity (kg /kg), C_e is the equilibrium concentration of the adsorbate (kg m^{-3}) and K_{ads} is the adsorption equilibrium constant (m^3 kg^{-1}). The plots of C_e/q_e versus C_e give a straight line of slope $1/q_\infty$ and intercept $1/(q_\infty K_{ads})$[35].

For single crystal surfaces, Langmuir isotherm describes the adsorption processes often quite well, especially at low and medium coverage. However, it fails if porous polycrystalline surfaces are used as adsorbents. Polycrystalline, heterogeneous surfaces are very important in practical heterogeneous catalysis, since they have a large surface area due to micro-, meso- or macropores. Among these solid are activated carbon, alumina, silica, zeolites or carbon nanotubes. Apparently, the Langmuir model is quite limited and seldom applicable for practical purposes -

in fact, the coverage dependence of the heat of adsorption must be taken into account as well as the possibility that more than just a single monolayer will adsorb[36].

2.3.3.2. Freundlich adsorption isotherm

The well-known Freundlich isotherm is often used for heterogeneous surface energy systems. The Freundlich equation generally givenas[34]:

$$q_e = K_F C_e^{1/n} \tag{2}$$

And a linear form of this expression is

$$\log q_e = \log K_F + \frac{1}{n} \log C_e \tag{3}$$

Where K_F is the Freundlich constant and n is the Freundlich exponent. K_F and n can be determined from the linear plot of $log\ q_e$ versus $logC_e$.

At present, Freundlich isotherm is widely applied in heterogeneous systems especially for organic compounds or highly interactive species on activated carbon and molecular sieves. The slope ranges between 0 and 1 is a measure of adsorption intensity or surface heterogeneity, becoming more heterogeneous as its value gets closer to zero. Whereas, a value below unity implies chemisorptions process where *1/n* above one is an indicative of cooperative adsorption. Recently, Freundlich isotherm is criticized for its limitation of lacking a fundamental thermodynamic basis, not approaching the Henry's law at vanishing concentrations[37].

2.3.3.3. BET adsorption isotherm

Brunauer-Emmett-Teller (BET) isotherm is a theoretical equation, most widely applied in the gas–solid equilibrium systems. It was developed to derive multilayer adsorption systems with relative pressure ranges from 0.05 to 0.30 corresponding to a monolayer coverage lying between 0.50 and 1.50. Its extinction model related to liquid-solid interface is exhibited as[37]:

$$q_e = \frac{q_s C_{BET} C_e}{(C_s - C_e)[1 + (C_{BET} - 1)(C_e / C_s)]} \quad (4)$$

Where C_{BET} is the BET adsorption isotherm (L/mg), C_s is the adsorbate monolayer saturation concentration (mg/L), q_s is the theoretical isotherm saturation capacity (mg/g) and q_e is the equilibrium adsorption capacity (mg/g), respectively.

Application of the B.E.T equation has shown it to be linear only over the range $p/p_o = 0.05$ to 0.35. The model fails at lower relative pressures due to adsorbent surface heterogeneity and at $p/p_o > 0.35$ where neglect of lateral interactions between neighbouring admolecules and the process of capillary condensation produce deviations in the plot.

The scientists studying isothermal adsorption kinetics in the first half of the 20th century focused mainly on the initial stage of adsorption, when the simultaneously appearing desorption can be safely ignored. Consequently, the related theoretical interpretation of isothermal adsorption kinetics neglected, as a rule, desorption term in the related theoretical expressions. Studies of desorption kinetics so rigorously developed[38]. Most adsorption research focused on the isotherm, kinetic, and thermodynamic processes. For the adsorption process, an analysis of the kinetic data is important because the kinetics describe the uptake rate of adsorbate, which in turn controls the resident time in the adsorbent-solution interface[39].

2.3.4. Adsorption kinetics

The Langmuir adsorption isotherm model is extensively applied in describing in several types of adsorption isotherms. This model was primarily proposed to describe adsorption in gas-solid systems. Later on it was adapted to liquid systems simply by replacing the partial pressure of the

adsorbate with its equivalent value in concentration. The Langmuir adsorption isotherm for liquid systems was represented by equation Eq. (1)[40]:

At a given temperature *T*, and fluid chemistry (pH, ionic strength etc.) the Langmuir parameters, q_∞, and K_{ads}, completely characterize an adsorbent-adsorbate-solvent system at equilibrium.

In technological applications the adsorption process is generally a part of a continuous process, and the processes are usually conducted under steady state conditions. For very high adsorption rates the steady state could be viewed as an equilibrium state, but in most cases the steady state remains far apart from the equilibrium. For this reason, together with the Langmuir equilibrium parameters (q_∞, and K_{ads}), knowledge about kinetic parameters of an adsorption system is essential for describing precisely the performance of an adsorption unit operating in technological processes.

An extensive study of the adsorption kinetics was done and several kinetic models including pseudo-first-order model, pseudo-second-order model, Weber and Morris sorption kinetic model, first-order reversible reaction model, external mass transfer model, first-order equation of Bhattacharya and Venkobachar, Elovich's model and Ritchies's equation[41] were used to predict the mechanism involved in the sorption process. Different literature analysis shows that though several kinetic models are available, except the pseudo-second-order model, no other model represents well the experimental kinetic data for the entire sorption period for most of the systems[42].

It is routine to fit equilibrium adsorption data from batch experiments to Eq. (1) to determine the Langmuir parameters (q_∞, and K_{ads}) of an adsorption system. However, to determine the kinetic parameters of both adsorption processes different authors use different equations. Lagergen pseudo-first[43] and pseudo-second[39] order kinetic model were widely used to fit the kinetic adsorption data Eqs. (5) and (6) respectively.

$$\frac{\mathrm{d}q_t}{\mathrm{d}t} = K_{1\mathrm{ads}}(q_e - q_t) \tag{5}$$

$$\frac{dq_t}{dt} = K_{2ads}(q_e - q_t)^2 \quad (6)$$

Where q_e is the amount of adsorbate adsorbed at equilibrium (mg/g), q_t is the amount of adsorbate adsorbed at time t (mg/g), K_{1ads}adsorption rate constant for first order (min^{-1}), K_{2ads}adsorption rate constant for second order (g mg^{-1} min^{-1}), and t is time of adsorption (min).

Equations (5) and (6) are empirical relations and any saturation type (irrespective of the process that it describes) can be fitted to them with some success and the rate constant K_{ads}, evaluated. However, even at the first glance it can be seen that the kinetic Eqs (5) and (6) have little to do with Eq (1)- the equation which is supposed to describe an adsorption system in equilibrium. In fact, the Langmuir parameters (q_∞, and K_{ads}) are constants for a given temperature and solution chemistry (pH, ionic strength etc.). They do not, by any means, depend on the initial concentration C_0, solution volume V or on the amount of adsorbent added W. thus the Langmuir parameters (q_∞, and K_{ads}) completely define an adsorption system in equilibrium.

Recently the adsorption process is viewed as a dynamic process of adsorption-desorption characterized by the rate constants $k_1$and $k_2$respectively, and these rate constants are independent of the operational parameters (C_0, W or V) of the adsorption process, as they should be. The kinetic equation for an adsorption-desorption process express the transient state of the process. The equilibrium state is viewed as a dynamic state of equal rate adsorption and desorption process, and characterized by an equilibrium constant K_{ads}, which is defined as equal to k_1/k_2. The kinetic equation reduces to Eq. (1) at equilibrium. Three parameters, q_∞, k_1 and $k_2$fully define both adsorption kinetics and adsorption equilibrium. These parameters can reproduce both isotherm and kinetic equations irrespective of the initial concentration of adsorbent dosage[40].

2.3.4.1. Lagergen Pseudo-first and Pseudo-second order Kinetic models

The rate of adsorption, r_{ads}, of a molecule onto a surface can be expressed in the same manner as any kinetic process. The Lagergen empirical equation proposed to describe the kinetics of solute sorption at the solid/solution interfaces has been the most widely used kinetic equation until now. This equation has also been called the pseudo-first order kinetic equation because it was

intuitively associated with the model of one-site occupancy adsorption kinetics governed by the rate of surface reaction. The pseudo-first order rate equation of Lagergen has long been widely applied and recently it was listed parallel to the pseudo-second-order (PSO) equation they had derived. Comparisons regarding the applicability to adsorption systems of these two (or more) equations have been done since then[44].A rate equation was developed which considered rates of ion-exchange adsorption in the exchange adsorption of ions from aqueous solutions by organic zeolites[45].

In an adsorption process, it is supposed that the rate (dq_e/dt) is proportional to the difference between the amount of adsorption at time t and the adsorption capacity of adsorbent ($q_e - qt$).

Kinetic models for sorption analysis, the Lagergen pseudo first order equation (Eq (5))[46]can be integrated in the range at $t = 0$, $q_t = 0$; $t = t$, and $qt = qt$:

$$\ln\left(1-\frac{q_t}{q_e}\right) = -K_{1\text{ads}}t \tag{7}$$

Eq. (5) is called the LFO equation or the PFO equation. Usually, $K_{1\text{ads}}$can be obtained from the slope of $\ln(q_e - q_t)$ vs. t.

The Lagergen pseudo second order kinetic model Eq. (6)[44]45can also be integrated for the boundary conditions $t = 0$to $t = t$ and $q_t = 0$to$q_t = q_t$, thus:

$$\frac{1}{(q_e - q_t)} = \mathrm{K}_{2\text{ads}}t + \frac{1}{q_e} \tag{8}$$

This equation can also further be rearranged as:

$$\frac{t}{q_t} = \frac{1}{K_{2\text{ads}}q_e^{\,2}} + \frac{t}{q_e} \tag{9}$$

Where $K_{2\text{ads}}$ is rate constant of second order adsorption (g mg^{-1} min^{-1}). The slopes intercepts of plot of t/q_t against t.

In recent years, linear regression correlation is frequently used to determine the best-fitting kinetic equation. An accuracy of a kinetic model is generally a function of the number of independent parameters, while its popularity in relation to the process application is an indicative of its mathematical simplicity. Likewise, linear regression is frequently used to determine the best-fitting kinetic equation primarily owing to its wide usefulness in a variety of adsorption data and partly reflecting the appealing simplicity of its equations. The linear least-squares method with linearly transformed kinetic rate equation has also been widely applied for confirming the experimental data using coefficients of determination. The kinetic equation giving a coefficient of determination closest to unity is considered to be the best fitting[47].

2.4. Thermalgravimetric Analysis

Thermalgravimetric Analysis is a technique in which the mass of a substance is monitored as a function of temperature or time as the sample specimen is subjected to a controlled temperature program in a controlled atmosphere. Upon heating a material, its weight increases or decreases.TGA measures a sample's weight as it is heated or cooled in a furnace. A TGA thermal curve is displayed from left to right. The descending TGA thermal curve indicates a weight loss occurred.

The following example is an illustration for the principle of TGA and since generally. A 15.013 mg sample of calcium carbonate was analyzed.

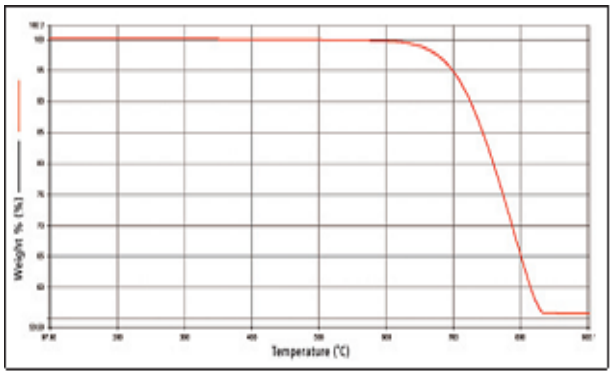

Fig. 2.4: The thermal decomposition of calcium carbonate

Upon heating calcium carbonate it undergoes a reaction where bound $CO_2$is released from the material and only calcium oxide remains after the experiment.

$$CaCO_3 \rightarrow CaO + CO_2$$

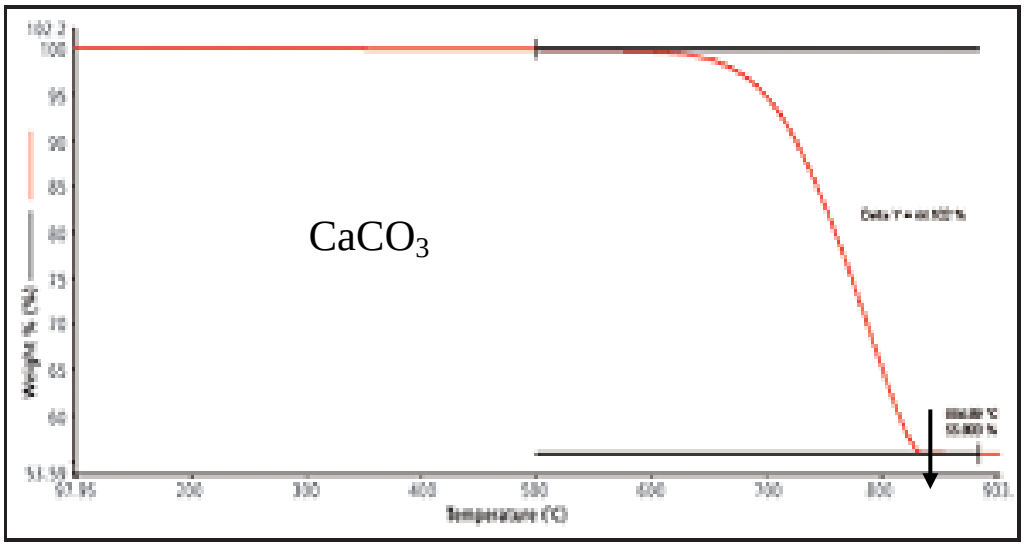

5

Fig. 2.5: Representative graph for analysis of TGA

3. OBJECTIVES

3.1. General objective

The general objective of this work is to study the kinetics of adsorption and desorption of ionic $[BMIM]^+$ $[Br]^-$ liquid into/out of mordenite using FT-IR and TGA.

3.2. Specific Objectives

- To synthesize and characterize $[BMIM]^+$ $[Br]^-$
- To characterize the interaction of ionic liquid and mordenite by FT-IR and TGA
- To study the kinetics of adsorption/desorption by quantifying the amount of ionic liquid into mordenite using CHN-elemental analysis
- To investigate the kinetics of adsorption/desorption using a model for adsorption kinetics

4. EXPERIMENTAL

4.1. Chemicals

Reagents bromobutane, 1-butylimidazole, 1, 1, 1-trichloroethane were all purchased from Sigma Aldrich, South Africa. All reagents were analytical grade and used without further purification. Mordenite was purchased from ZEOLYST, USA, with case number (CBV 21A), SiO_2/AlO_3 mole ratio of 20, ammonium cation, surface area of 500 m^2/g and Na_2O weight of 0.08.

4.2. Procedure

4.2.1. Synthesis of 1-Butyl-3-methylimidazolium bromide

$[BMIM]^+[Br]^-$ was synthesized using a procedure reported[48]. 40 ml of 1-butylimidazole and 65 ml of bromobutane were added to a 100 ml round-bottomed flask fitted with a reflux condenser at 70 °C for 24 hr. Then 1,1,1-trichloroethane (TCE) was added and the mixture was stirred until the two phases were formed. The top phase contains unreacted starting material. The bottom phase was decanted and washed with 1,1,1-trichloroethane thoroughly. This step was repeated three times to remove unreacted material from the bottom phase. The remaining solvent was evaporated using rotary-evaporator at 100 °C for about 2 hr. The resulting ionic liquid was characterized by ^{1}H-and ^{13}C NMR using a Bruker 400MHz NMR spectrometer.

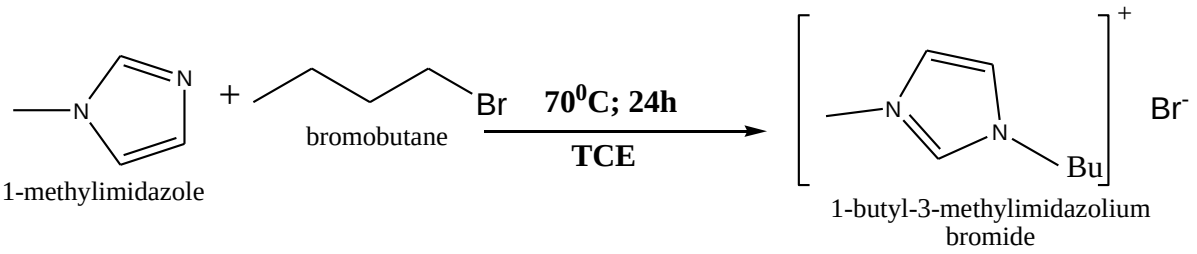

Scheme 4.1: Synthesis of 1-butyl-3-methylimidazolium bromide

^{1}H NMR of the neat ionic liquid sample (d-chloroform, ppm) contains peaks at δ: 10.43 (s), 8.21 (d), 4.63 (t), 4.15 (s), 3.53 (s), 2.01 (p), 1.39 (q), and 0.94 (t). ^{13}C NMR results (ppm) include: δ: 207.93, 138.41, 126.23, 49.66, 36.3, 33.41, 32.09, 20.60, and 14.74. The result obtained excellently matches with the literature[49]reported values confirming the purity of the synthesized

ionic liquid $[BMIM]^+$ $[Br]^-$. The synthesized ionic liquid was then used in the subsequent experiments.

4.2.2. Activation of Mordenite

Mordenite was pretreated by calcination in order to transform the terminal ammonium groups to hydroxyl groups and to remove possible organic impurities from the pore. A furnace CARBOLITE, model ELF was used at a temperature of 550 °C for 6 hr. An initial ramp rate was applied at a rate of 10 °C/min.

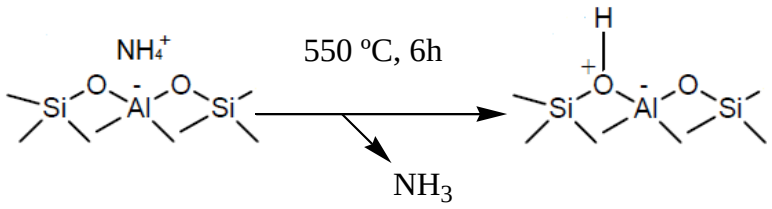

Scheme 4.2: schematic representation of calcination of mordenite

4.2.3. Adsorption of [BMIM] [Br]

1-butyl-3-methylimidazolium bromide and mordenite (A proportion of 32:1 in mass**)** were added into a round-bottomed flask fitted with a magnetic stirrer. The flask was heated using an oil bath and a hot plate. The temperature was adjusted to 100 °C. The round-bottomed flask was covered with a stopper and the mixture was left for 48 hr to react. Samples were taken at different times. Every sample was immediately cooled by mixing it with 30 ml of distilled water. The solid was separated by centrifugation and the supernatant was discarded. The solid sample was then washed with 20 ml of distilled water and centrifuged. The washing procedure was repeated three times to assume that no free ionic liquid remains. The remaining solid is dried in an oven at 60 °C. Thereafter, adsorption experiments were done for calcined and not calcined mordenite in the same fashion.

4.2.4. Desorption of [BMIM] [Br]

A batch of $[BMIM]^+$ $[Br]^-$ in mordenite is prepared to be used as starting point for desorption experiments. 0.04 g of this initial batch and 40 g water were placed into a round-bottomed flask which is fitted with a condenser. The flask was kept at 90 °C using oil bath with a hot plate and

continuously stirred. The reaction was carried out at different times up to 48 hr. The sample was washed, and decanted washing was done by the same procedure described previously.

$$\mathbf{MOR} \xrightarrow[\mathbf{100\ ^0C;\ 48h}]{\mathbf{[BMIM]\ [Br]}} \mathbf{MOR.\ [BMIM]\ [Br]}$$

Scheme 4.3: Adsorption of $[BMIM]^+[Br]$into mordenite

$$\mathbf{MOR\ ([BMIM]\ [Br])} \xrightarrow[\mathbf{90\ ^0C,\ 0\text{-}48h}]{\mathbf{H_2O}} \mathbf{MOR}$$

Scheme 4.4: Desorption of $[BMIM]^+[Br]^-$ from mordenite

4.3. Characterization Methods

4.3.1. Thermalgravimetric Analysis

Thermalgravimetry is based on the continuous recording of mass variation of a sample specifically related to temperature change. It can be used to analyze organic, inorganic and synthetic materials.

Thermal gravimetric analyses were measured using Perkin Elmer TGA7 instrument with a heating rate of 10 °C/ min under air flow.

4.3.2. Infrared Measurements

Infrared spectra were recorded using Perkin-Elmer spectrum 400 FT-IR spectrometer, USA, in the spectral range 700 – 4000 cm^{-1}. Attenuated total reflectance (ATR) was used for measuring the pure ionic liquid. Solid samples (zeolites with or without ionic liquids in the pore) were measured by transmittance mode diluting them in pellets of KBr.

4.3.3. Elemental Analysis

CHNS elemental analyzers provide a means for the rapid determination of carbon, hydrogen, nitrogen and sulfur in organic matrices and other types of materials. Elemental analysis were measured with EA 1112 Flash CHNS/O- analyzer with a carrier gas flow rate of 120 ml/min,

reference flow rate 100 ml/min, oxygen flow rate 250 ml/min; furnace temperature of 900 °C and oven temperature of 75 °C. Sample was loaded with a tin capsule.

In the combustion process (furnace at ca. 900 °C), carbon is converted to carbon dioxide; hydrogen to water; nitrogen to nitrogen gas/ oxides of nitrogen and sulfur to sulfur dioxide.

The combustion products are swept out of the combustion chamber by inert carrier gas such as helium and passed over heated high purity copper. The function of this copper is to remove any oxygen not consumed in the initial combustion and to convert any oxides of nitrogen to nitrogen gas.

Detection of the gases is carried out using a GC separation followed by quantification using thermal conductivity detector. Quantification of the elements requires calibration for each element by using high purity 'micro-analytical standard' compounds. Acetanilide, sulfanilamide, and benzanilide were used. The calibration curves consisted on six points, two points for every standard.

5. RESULTS AND DISCUSSION

Kinetics of adsorption/desorption of 1-butyl-3-methylimidazolium bromide were studied using TGA, FT-IR and CHN elemental analysis. The kinetics was analyzed using Lagergen pseudo first and pseudo second kinetic models.

5.1. Characterization of Samples (TGA and FT-IR)

Figure 5.1shows the thermogram obtained for the pure ionic liquid ($[BMIM]^+$ $[Br]^-$) and the pure mordenite.

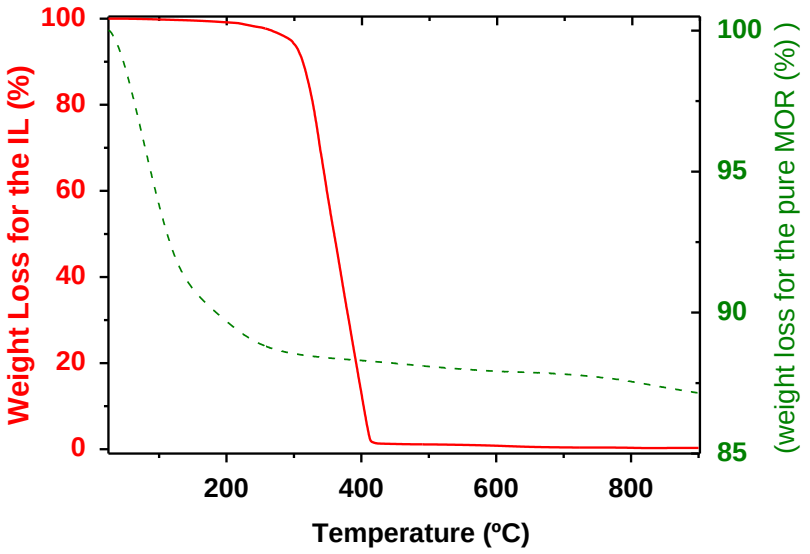

Fig. 5.1: Thermogram of pure ionic liquid (solid line) and pure calcined Mordenite (broken line)

The TGA curve of ionic liquid (solid line) showed that the decomposition of the organics started around 300 °C, and was complete in the range 400 – 420 °C. Generally, ionic liquids are thermally stable up to 300 °C[49] and the result obtained from thermalgravimetric analysis is consistent with the thermal behaviour of common ionic liquids. The rate of decomposition of organics is very fast as it is shown in the TGA curve above. At about 400 °C, only 1.558% of ionic liquid remains. For pure calcined mordenite (broken line), there is a rapid weight loss in between 100 –200 °C, which is due to the weight loss of water from the crystal.

The TGA curve obtained for ionic liquid adsorbed into mordenite together with the thermogram (TGA curve) of pure ionic liquid, for comparison purpose, is shown below (Fig. 5.2)

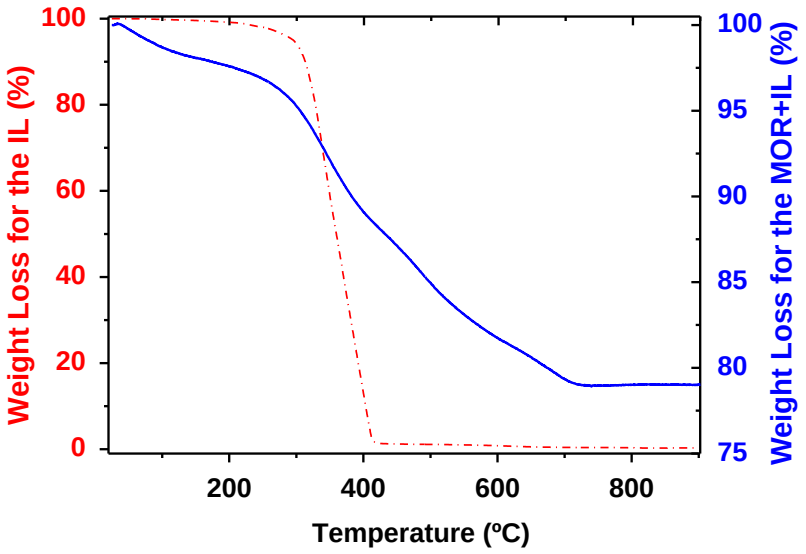

Fig.5.2: Thermogram of $[BMIM]^+$ $[Br]^-$ with mordenite (solid line) and pure $[BMIM]^+[Br]^-$(broken line).

From the TGA curve (Fig. 5.2) it can be observed that in ionic liquid adsorbed into mordenite (solid line) there is approximately 4% weight loss between 100 °C and 200 °C, which is attributed to loss of water. The second decomposition phase began at similar temperature to the thermal decomposition of the pure ionic liquid (325 °C), and then continued slowly, suggesting that the observed weight loss is due to the organic matter present inside the pore of mordenite, which is related to the confinement effect of mordenite stabilizing the ionic liquid inside its pore. The overall weight loss obtained from TGA was about 17%, and the result clearly indicates the adsorption of ionic liquid into mordenite.

The sample was further characterized using FT-IR. Figure 5.3 shows IR spectra of pure [BMIM] [Br] obtained using ATR and Mordenite with ionic liquid ([BMIM] [Br]).

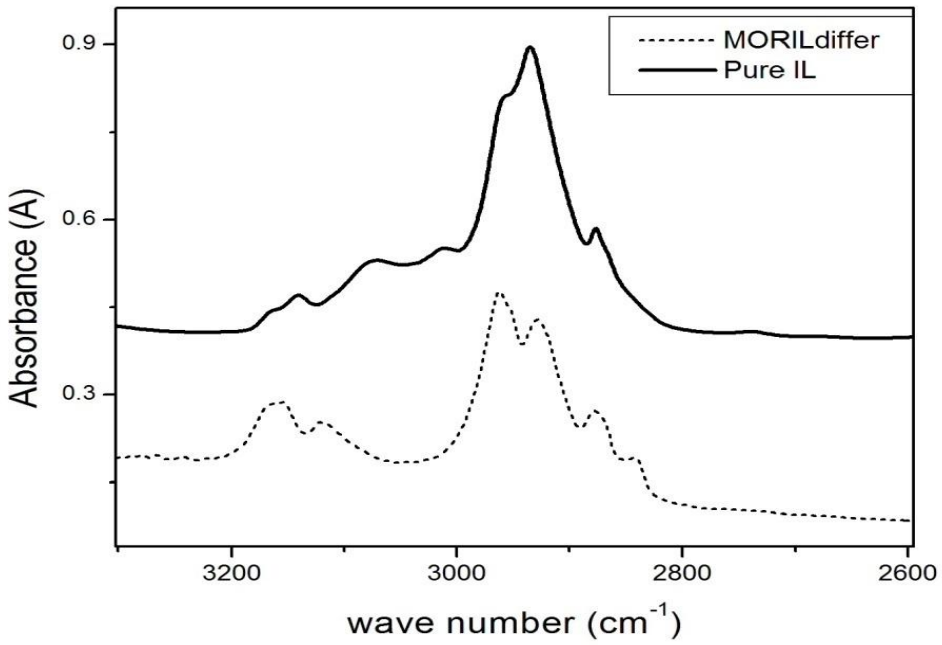

Fig.5.3. FT-IR spectrum of pure ionic liquid (1-butyl-3-methylimidazolium bromide) (solid line) and mordenite with ionic liquid (broken line)

The spectra of pure ionic liquid (solid line) and ionic liquid intercalated into mordenite (broken line) exhibited similar spectral properties in the range 2600 – 3300 cm^{-1}. However, there is an observable difference at the maximum absorption range 2900 – 3000 cm^{-1}, in which in the band shapes look mirror images to each other. In order to investigate the origin of this difference, series of concentration dependent spectra were recorded. The results are presented in (Fig. 5.4). The spectrum for the diluted solution (conc 5) resembles the spectrum of the ionic liquid depicted in Fig. 5.3 (IL diluted). When the concentration was successively increased, the band at higher energy intensified at the expense of the band at lower energy. The spectrum obtained for the concentrated solution is fairly similar to the spectrum obtained for the ionic liquid intercalated into mordenite (broken line). Therefore, the observed difference in the band shapes is attributed to the concentration effect, and suggests that a significant amount of ionic liquid is adsorbed in mordenite.

.

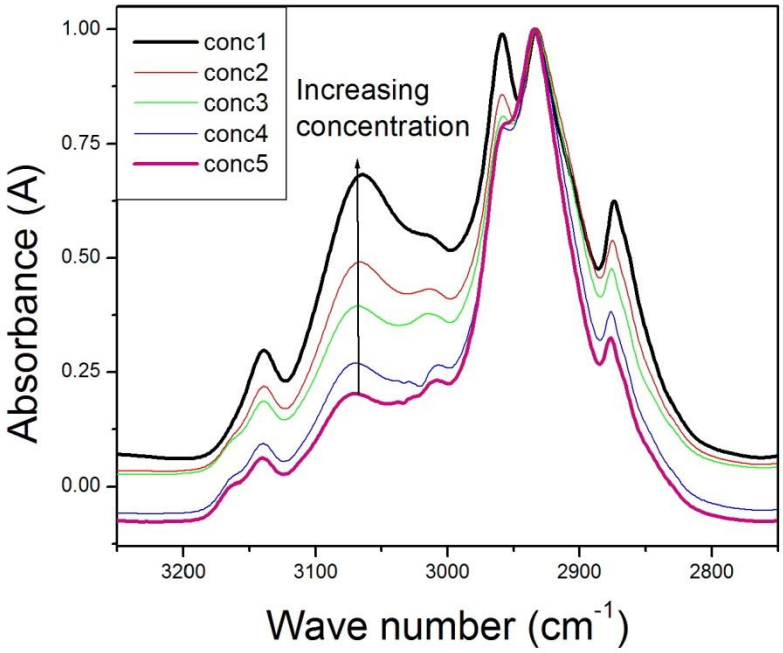

Fig.5.4: concentration effect in ionic liquid with chloroform. Conc 1: most concentrated; conc 5: most diluted.

5.2. CHN Elemental Analysis

In the analysis elemental of 1.2 to 2% for N_2 and 4 to 6% for C were recorded. Taking into account the empirical formula of $[BMIM]^+$ $[Br]^-$($C_8H_{15}N_2Br$), an increment of one mass unit of N_2 would mean 7.82 mass units of IL incorporated. In Fig.5.5 the result obtained from the elemental analysis at different time interval of adsorption and desorption experiments is presented.

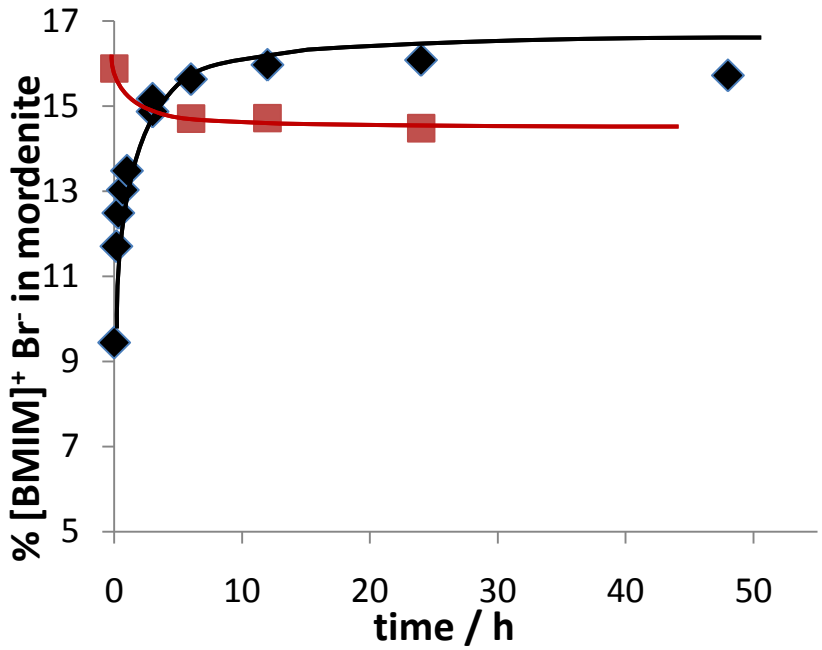

Fig.5.5: (—◆—): adsorption of [BMIM] [Br] into mordenite. (—■—): Desorption of [BMIM] [Br] from mordenite (calcined mordenite) (eye guide).

From Fig. 5.5, it can be observed that the amount of ionic liquid adsorbed into mordenite increases with time, and the rate of adsorption of $[BMIM]^+$ $[Br]^-$ into mordenite was fast and reached equilibrium of 16% at about 10 hr. The amount observed is in good agreement with the result obtained from TGA (17%). The rate of desorption was similar to that of adsorption. However, the amount desorbed was only 9%, indicating that most of the ionic liquid stays adsorbed.

Similar rate of adsorption property was obtained for the uncalcined mordenite. However, there was a signification difference in the amount of adsorbed ionic liquid was obtained (Fig. 5.6).

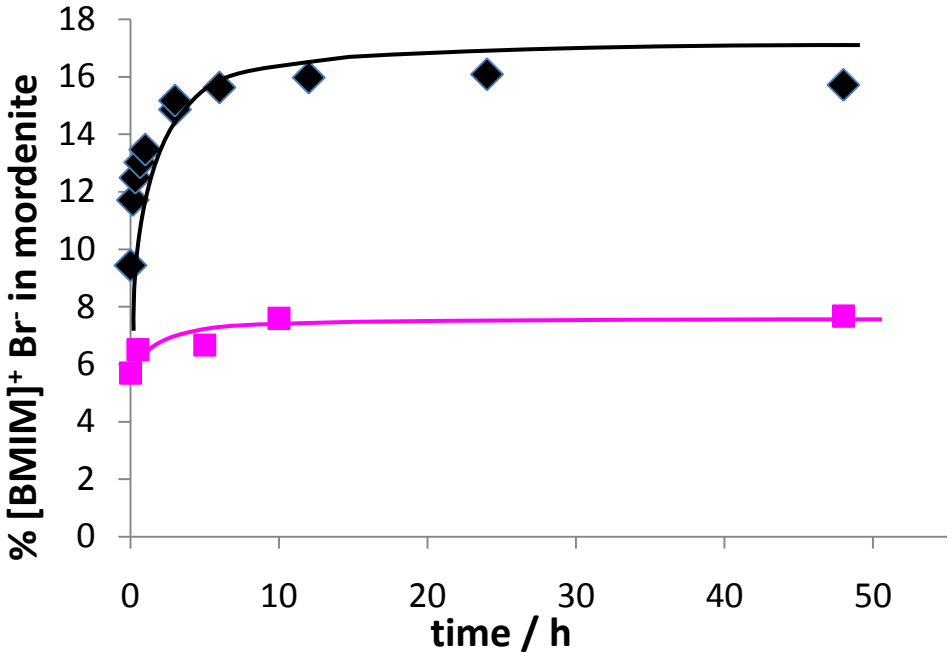

Fig.5.6: (—◆—): adsorption mass of [BMIM] [Br] into calcined mordenite. (—■—): adsorption mass of [BMIM][Br] into uncalcined mordenite (subtracting the blank non-calcined mordenite) (eye guide).

The apparent larger amount of adsorbate in the case of calcined mordenite is due to the fact that it is higher presence of N_2 (typical values between 2.6 to 3%), and also the pure mordenite (starting material) contains 2.1% of N_2 itself (due to the presence of NH_4^+ groups). If this amount is subtracted from every sample lower values for N_2 are obtained for the uncalcined than for the calcined mordenite. In order to further explain this, additional analysis was conducted.

Additional information about the adsorption mechanism can be obtained by considering nitrogen to carbon ratio **C:N** (in mole. From the elemental analysis it was calculated the **C:N** ratio to be 3.7 ± 0.3for calcined mordenite, which is consistent with the amount $[BMIM]^+[Br]^-$incorporated into the pores of mordenite (empirical formula of $[BMIM]^+[Br]^-$ is $C_8N_2H_{15}Br$). Whereas the calculated **C:N** ratio for ionic liquid adsorbed into uncalcined mordenite is found be 8.8 ±0.7, that is one nitrogen for every eight carbons. This value represents the exchange of one mole of $[BMIM]^+$ NH_4^+.

For every gram of nitrogen there is 7.82 g of [BMIM] [Br] for the case of calcinedmordenite, however, for non-calcined mordenite for every gram of nitrogen there is only 4.32 g of $[BMIM]^+$.

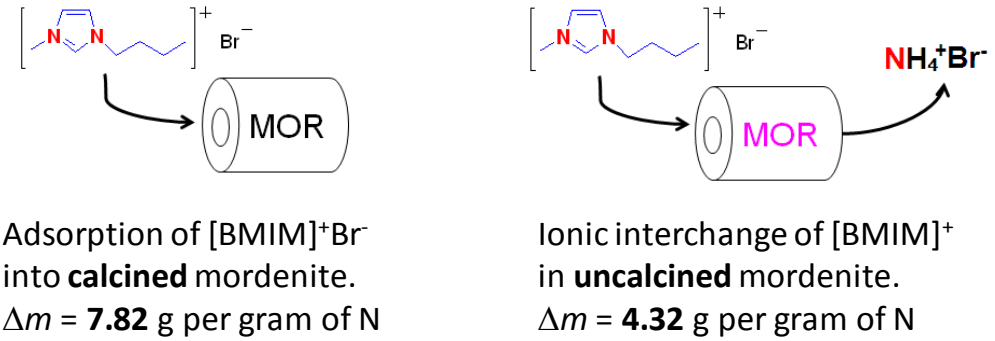

Fig.5.7: adsorption mechanism of calcined and uncalcined mordenite

Taking into account the above discussed considerations one can calculate the mass adsorption in non-calcined mordenite. As shown in Fig.5.6, it is evident that the amount in non-calcined mordenite (the blank is subtracted in non-calcined case) is lower than the adsorption in calcined one, assuming that only $[BMIM]^+$ is the adsorbed moiety.

Considering that for non-calcined mordenite the adsorption occurs via a cation exchange between NH_4^+ and $[BMIM]^+$(only $[BMIM]^+$ is adsorbed into the pore), the adsorbed mass for non-calcined is less than that of calcined mordenite, as shown in figure 5.6. This is expected because the mass of Br is large (it accounts for more than 1/3 of the IL mass). However, if we calculate the inclusion of $[BMIM]^+$ in mol (by either adsorption or ionic interchange), we obtain a similar amount included into mordenite for both calcined and non-calcined (figure 5.8) i.e. approximately the same amount of $[BMIM]^+$ fit into the pore, consistent to the fact that the size of the pores is the same.

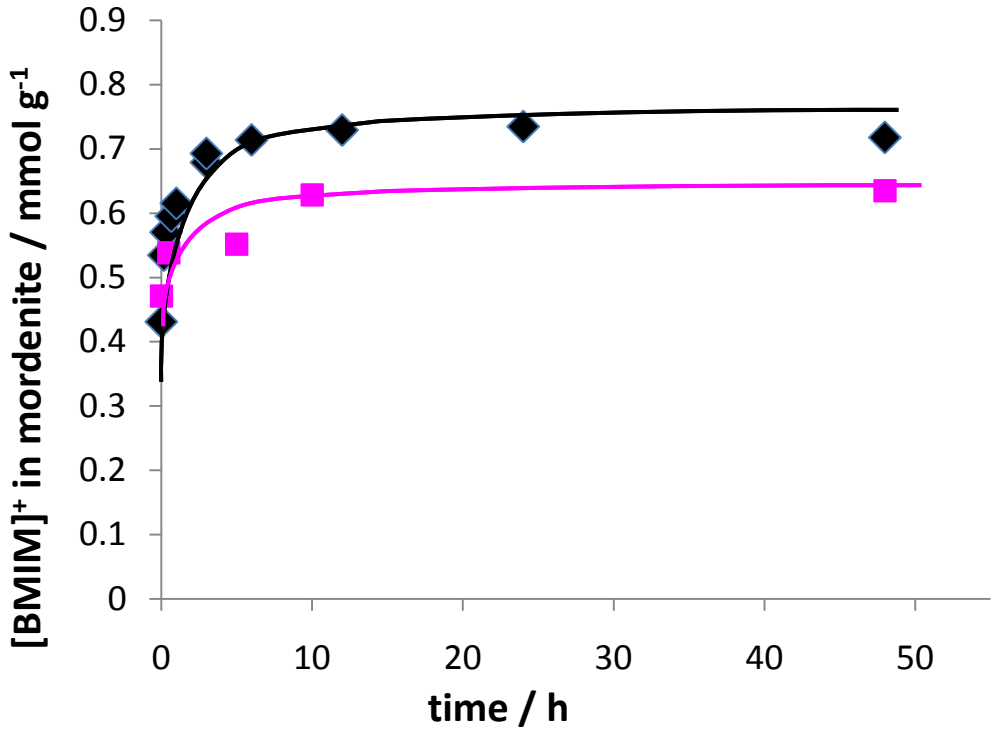

Fig. 5.8: (—◆—): adsorption mol of [BMIM] [Br] into mordenite; (—■—): adsorption mol of [BMIM] [Br] into uncalcined mordenite (the blank non-calcined mordenite is not subtracted) (eye guide).

5.3. Kinetics of Adsorption

Several adsorption models were tested and the Lagergen pseudo-first order and pseudo second order kinetic models proved to fit best the experimental data. The following figure is a linear fit of experimental data using Lagergen pseudo first order kinetic model Eq. 7:

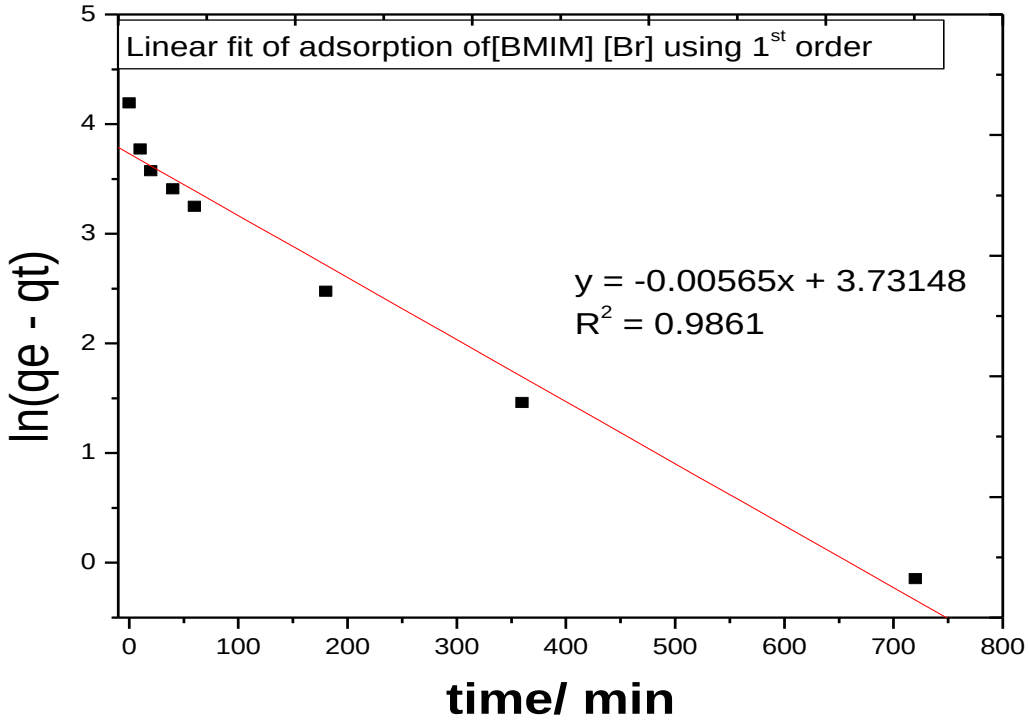

Fig.5.9: Linear fit of experimental data using pseudo first order kinetics for adsorption of [BMIM] [Br] into mordenite

From Lagergen pseudo first order kinetics model the regression correlationR^2 is 0.986 and $K_{1ads}$is 0.00565 min-1 were obtained. In closer looking of the fit the data points at the start and end are above the fit whereas in the middle below the fit, though the regression correlation obtained from this fitting is close to one, implying the pseudo- first order may not be the appropriate model. In addition, the calculated value for q_e (about 40 mg/g) is not consistent with the experimental value of 160.8 mg/g. Therefore, the adsorption of $[BMIM]^+$ $[Br]^-$ into mordenite was also analyzed using Lagergen pseudo second order kinetic model (Eq. 9).

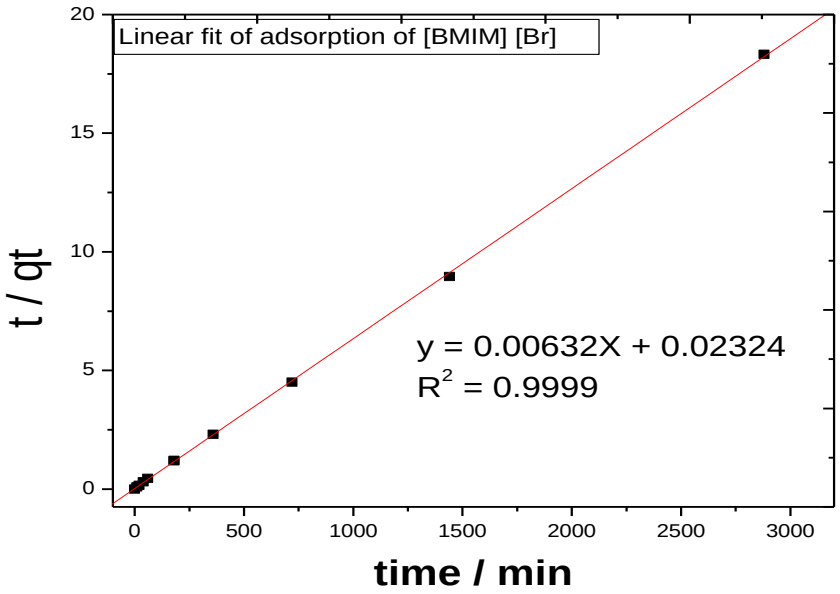

Fig.5.10: Linear fit of experimental data using pseudo second order kinetics for adsorption of [BMIM] [Br] into mordenite.

The regression correlation R^2 obtained from Lagergen pseudo second order kinetic model is 0.9999, and also the data are statistically go with the fit, suggesting that Lagergen pseudo-second order kinetic model better appropriate in fitting the experimental data for adsorption of $[BMIM]^+$ [Br] into mordenite. Using the model, the calculated value for q_e was 158.2 ± 0.8 mg/g which is very close to the experimentally obtained value of 160.8 mg/g. The rate constant was also calculated from the zero intercept (Eq. 9). However, the zero intercept is $2.3\times10^{-4} \pm 5\times10^{-4}$ mg/g. Since the standard deviation of the intercept is much larger than the value itself, it is a meaningless to try to calculate the rate constant from this fit. Therefore, an alternative fitting method, consisting of fitting $1/(q_e - q_t)$ against t, as given in Eq. 10 was employed. The slope of the curve is the value for K_{2ads}.

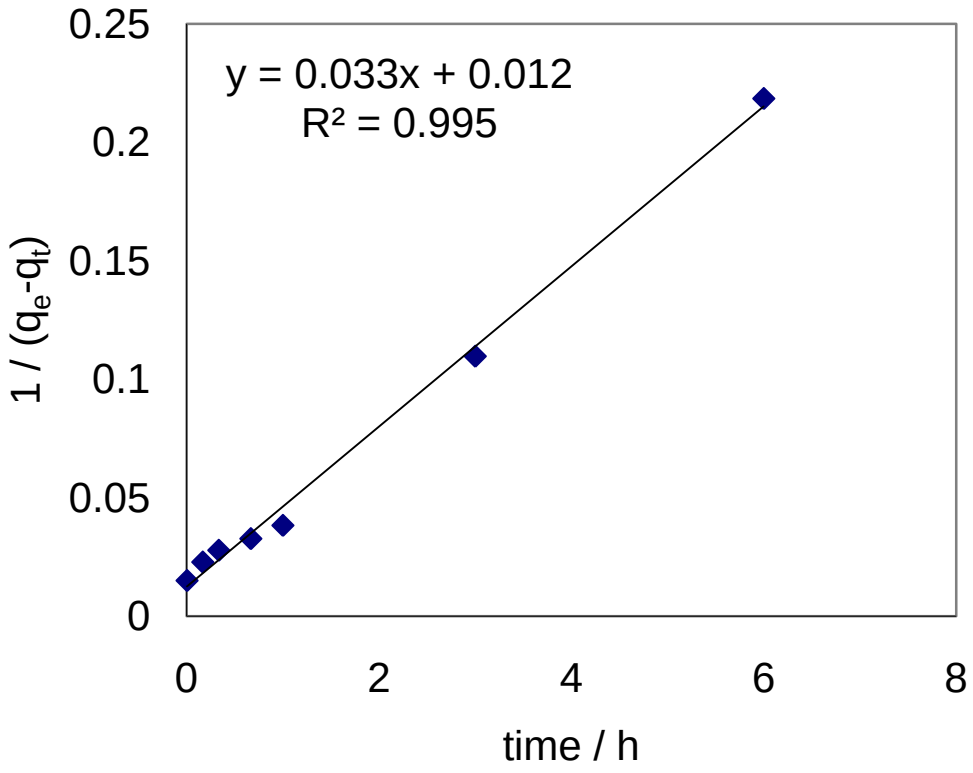

Fig. 5.11: linear fit of experimental data using Pseudo second order kinetics for adsorption of $[BMIM]^+[Br]^-$ into mordenite ($1/(q_e - q_t)$ against t)

From the fit (Fig. 5.11), a correlation parameter $R^2 = 0.995$ was obtained, confirming the validity of the fit. Thus, the value for K_{2ads} could accurately be determined to be 0.033 ± 0.001 g/mg. Therefore, it can be concluded that the overall adsorption process of $[BMIM]^+[Br]^-$ into mordenite obeys second order kinetic model.

6. SUMMARY AND CONCLUSIONS

The kinetics of adsorption and desorption of the ionic liquid $[BMIM]^+[Br]^-$ into/from calcined and non-calcined mordenite was studied using TGA, FT-IR and CHNS elemental analyzer. In addition, the adsorption process was also studied using pseudo first and pseudo second order Lagergen kinetic models.

The thermal stability was determined over a temperature range from 25 – 900 °C. The first thermal decomposition started at 100 °C – 200 °C which was likely to be due to water loss. The second decomposition started around 315 °C. There is no further decomposition until the thermal decomposition of mordenite.

Adsorption of $[BMIM]^+[Br]^-$ into mordenite was characterized using FT-IR. The spectra of the pure ionic liquid and ionic liquid intercalated into mordenite exhibited a similar spectral band in the range between 2900 – 3000 cm^{-1}, confirming the adsorption of the ionic liquid into mordenite.

CHN elemental analysis was used for quantitative determination of kinetics of adsorption and desorption of $[BMIM]^+[Br]^-$ in mordenite. The adsorption of $[BMIM]^+[Br]^-$ increased with time and reached equilibrium about 16% of ionic liquid. The rate of adsorption of $[BMIM]^+[Br]^-$ into mordenite occurred relatively fast, within an hour, but the rate of desorption occurs much slower (only 9%), implying that most of the ionic liquid stay inside the pores of mordenite. This may adversely affect the catalytic property of the zeolite.

CHN elemental analysis also was also employed to extract additional information about the mechanisms of adsorption, in which, in contrary to the calcined mordenite, in uncalcined mordenite it was found that there is an ion exchange between NH_4^+ $[BMIM]^+[Br]^-$.

Lagergen pseudo second order highly fits with the experimental data. The regression correlation obtained from the Lagergen pseudo second order kinetic model is 0.9999 and the rate constant is 0.033 ± 0.001g mg^{-1} min^{-1}. q_e calculated was found to be 158.2 ± 0.8 mg/g, which is very close to the experimental value 160.8 mg/g. The overall adsorption process obeys second order kinetic model.

7. REFERENCES

[1] D.J. Liu and E. Y.-X. Chen. *Biomass and Bioenergy*.**2013**, 48, 181-190.

[2] N. Hui; S. JinLiang; H. MinQiang; Y. DeZhong; F. HongLei; and H. BuXing. *Sci China Chem*. **2013**, 56 (11), 1578–1585.

[3] G. De Cremera; E. Bartholomeeusena; P. P. Pescarmonaa; K. Lina; D. E. De Vosa; J. Hofkensb; M. B.J. Roeffaersb; and B. F. Sels. *Catal.Today*.**2010**, 157, 236–242.

[4] L. Ayele; G. Dadi; W. Mamo; Y. Chebude; and I. Diaz. *Bull. Chem. Soc. Ethiop*. **2014**, 28(1), 1-8.

[5]WondimagegneMamo. "Conversion of Glucose into 5-hydroxymethylfurfural Using Zeolite Catalysis": PhD Progress Report, Department of Chemistry, Addis Ababa University, 2013.

[6] K. S. S. B. Thomas Heinze. *Macromol.Biosci*.**2005,** 5, 520-525.

[7]R. J. Marcel; D. M. Alonso; M. A. Mellmer; and J. A. Dumesic. *Green Chem*. **2013**, 15, 85-90.

[8] L. Hu; G. Zhao; W. Hao; X. Tang; Y. Sun; L. Lin; and S. Liu. *RSC Adv.*, **2012**, 2, 11184–11206.

[9] A. Godelitsas; P. Gamalestsos; and M. Roussos-Kotsis. *Eur. J. Mineral*. **2010**, 22, 797-811.

[10] L. Zhang; C. Chmelik; A. N. C. Van Laak; J. Karger; P. E. de Jongh; and K. P. de Jong. *Chem. Commun*. **2009**, 6424-6426.

[11] C. Moreau; R. Durand; S. Razigade; J. Duhamet; P. Faugeras; P. Rivalier; P. Ros; G. Avignon. *Appl*. *Catal. A: Gen.* **1996**, 145, 211.

[12] S. Sugden and H. Wilkens. *J. Chem. Soc*. 1929.

[13] T. Welton. *Chem. Rev*. **1999**, 4, 2071-2083.

[14]M. Freemantle. An Introduction to Ionic Liquids.*Royal Society of Chemistry*.**2010.**

[15] S. Keskin; D. Kayrak-Talay; U. Akman; and O. Hortaçsu. *J. Supercr.Flui*.**2007**, 43, 150–180.

[16] P. Wasserscheid and T. Welton. Ionic liquids in synthesis. 2nd ed. Weinheim: *Wiley-VCH*. **2008**.

[17] S. Zhang; N. Sun; X. He; X. Lu; and X. Zhang.*J. Phys. Chem. Ref. Data*. 2006, 35 (4), 1475-1517

[18]A. I. Mohammad. Green Solvents ii: Properties and Applications of Ionic Liquids. *Springer*. **2012**.

[19] R. P. Swatloski; S. K. Spear; J. D. Holbrey; and R. D. Rogers.*J. Am. Chem. Soc*. **2002**, 124, 4974-4975.

[20] R. Rinaldi; R. Palkovits; and F.Schüth. *Angew. Chem. Int. Ed*. **2008**, 47, 8047-8050.

[21] V. I. Parvulescu and C. Hardacre.*Chem. Rev*.**2007**; 107, 2615-2665.

[22] (a) N. Sun; H. Rodriguez; M. Rahman; R. D. Rogers. *Chem. Commun*. **2011**, 47, 1405-1421;

(b) A Pinkert; K. N. Marsh, Pang S; and M. P. Staiger. *Chem. Rev.* **2009**; 109, 6712-6728.

[23] S. Ntais; A. M. Moschovi; V. Dracopoulos; and V. Nikolakis. *ECS Transactions*.**2010**, 33(7), 41-47.

[24] S. M. Aulerbach; K. A. Carrado; and P. K. Dutta.Handbook of Zeolite Science and Technology.*Marel Decker, Inc*. **2003**.

[25]M. Moliner. *ISRN Materials Sci*.**2012**, 1-24.

[26] P. A. Jacobs; E. M. Flanigen; J. C. Jansen; and H. Van Bekkum.Introduction to Zeolite Science and Practice. *Elsevier*. **2001**.

[27] S. G. Wettstein; D. M. Alonso; E.I Gurbuz and J.A Dumesic.*Current Opinion in Chem. Eng*.**2012**, 1, 218–224.

[28] E. Taarning; C. M. Osmundsen; X. Yang; B. Voss; S I. Andersena; and H. Claus. *Energy Environ. Sci*. **2011**, 4, 793-804.

[29] G. De Cremera; E. Bartholomeeusena; P. P. Pescarmonaa; K. Lina; D. E. De Vosa; J. Hofkensb; M. B.J. Roeffaersb; and B. F. Sels. *Catal.Today*. **2010**, 157, 236–242.

[30] R. Cai; M. Sun; Z. Chen; R. Munoz; C. O'Neill; D. E. Beving; and Y. Yan. *Angew.Chem. Int. Ed*. **2008**, 47, 525–528.

[31] McGraw-Hill. Dictionary of Chemistry. 2nd Ed.*McGraw-Hill Companies, Inc*. New York. **2003**

[32] B. K. Dutta. Principles of Mass Transfer and Separation Process.*Asoke K. Ghosh, PHI Learning Private Limited, M-97*. New Delhi. **2009**.

[33] H. G. Karge and J. Weitkamp.Adsorption and Diffusion. *Springer*. **2008**.

[34]F.O. Okeola and E.O. Odebunmi. *Adv. in Nat. Appl. Sci*. **2010**, 4(3), 281-288.

[35]M. Özacar. *Adsorption*.**2003**, 9, 125–132.

[36] J.W Sutherland. In Porous Carbon Solids; Bond. R. L., Ed.; *Academic Press*: London, **1967**.

[37] K.Y. Foo and B.H. Hameed. *J. Chem. Eng*. **2010**, 156, 2–10.

[38] W. Rudzinski and T. Panczyk. *Adsorption*. **2002**, 8, 23–34.

[39] J. Lin and L. Wang. *Front. Environ. Sci. Engin. China*. **2009**, 3(3), 320–324

[40] A. Islam; M. R.Khan; and M. S. I. Mozumder. *Chem. Eng. Technol*. **2004**, 27(10), 1095-1098.

[41] J. Febrianto; A.N. Kosasiha; J. Sunarsob; Y. Jua; N. Indraswati; S. Ismadji. *J Hazard Mater*.**2009**, 162, 616–645.

[42]Y.S. Ho. *J. Hazard. Mater*.**2006**, 136 (B), 681–689.

[43] R.L. Tseng; F. C. Wu; and R. S. Juang. *J. Taiwan Institute of Chem. Eng*. **2010**, 41, 661–669.

44 W. Rudzinski and W. Plazinski. *J. Phys. Chem. B*.**2006**, 110(33), 16514-16525.

[45] Y.S. Ho and G. McKay. *Process Bio.Chem*. **1999**, 34, 451–465.

[46] M. Francisco; A.N. Mlinarc; B. Yoo; A.T. Bell; and J. M. Prausnitz. *J. Chem. Eng.***2011**, 172, 184–190.

[47] S. Chowdhury and P. Saha. *J. IIOAB*. **2010**, 1 (3); 1-7.

[48] T. Ståhlberg, W. Fu; M. Woodley; and A. Riisager. ChemSus Chem. **2011**, 4, 451–458.

[49] P.N. Tshibangu; S.N. Ndwandwe; and E.D. Dikio. *Int. J. Electrochem. Sci*. **2011**, 6, 2201-2213.